PRZEGLĄD ELEKTROTECHNICZNY

Ukazuje się od 1919 roku

3'18

Organ Stowarzyszenia Elektryków Polskich • Wydawnictwo SIGMA-NOT Sp. z o.o.

Paolo DI BARBA[1], Maria Evelina MOGNASCHI[1], Marco BULLO[2], Fabrizio DUGHIERO[2], Michele FORZAN[2], Sergio LUPI[2], Elisabetta SIENI[2]

University of Pavia (1), University of Padova (2)

doi:10.15199/48.2018.03.01

Field models of induction heating for industrial applications

Abstract. *— In the paper, a benchmark in the area of induction heating is revisited in order to test methods and codes of field analysis in a comparative way. In particular, the transient thermal analysis of a steel-made cylindrical billet is considered: the coupled-field problem is non-linear and multiphysics. After briefly describing the benchmark problem, the results from a finite-difference solver and two finite-element solvers are presented and compared.*

Streszczenie. *W artykule przywołano wzorzec (benchmark) w obszarze grzania indukcyjnego w celu porównawczego przetestowania metod I kodów komputerowych w analizie pola. W szczególności skupiono się na analizie cieplnej stanów przejściowych stalowych wkładów cylindrycznych. Problem pól sprzężonych jest nieliniowy i wielofizyczny. Po krótkim opisania problemu wzorcowego zaprezentowano i porównano wyniki otrzymane z programów różnic skończonych I elementów skończonych. (**Modele polowe grzania indukcyjnego w zastosowaniach przemyslowych**).*

Keywords: Induction heating, multiphysics problem, magnetic-steel billet, benchmark problem.
Słowa kluczowe: grzanie indukcyjne, problem wielofizyczny, wkład ze stali magnetycznej, problem wzorcowy

Introduction

In the community of computational electromagnetics, the set of benchmark problems proposed by the TEAM (Testing Electromagnetic Analysis Methods) series of workshop is a reference for testing numerical methods in a comparative way [1]-[2]. Nevertheless, there is a lack of problems specifically focused on induction heating devices, as far as numerical modelling is concerned. More generally, in the past some benchmarks of induction heating was proposed, but the attention was focused rather on the inverse problem [3]–[7] related to the optimal design of the power inductor than on the direct problem of field analysis [8], [9]. In fact, in computational induction heating, analysis problems are challenging because they involve different physical domains; therefore, the development of non-linear coupled-field models and the consequent choice of suitable solvers is mandatory [8]–[10]. Too often numerical solvers, like e.g. finite-element solvers which are commercially available, are used by designers as general-purpose black boxes.

Moving from this background, it was proposed to define a benchmark of coupled-field analysis [5]; the problem is taken from industrial applications of induction heating: it deals with the transient thermal analysis of a steel-made cylindrical billet, subject to the changing magnetic field of a multi-turn winding. It is a clear example showing that stiff analysis problem can originate even in the case of very simple geometries.

Benchmark description: the device

The device under study is composed of an inductor winding and a cylindrical billet; winding and billet are coaxially located.

A. Geometry

The billet has a radius r and height h. The inductor is made of 20 hollow circular turns, connected in series; each of them has height hc and width wc, while their radial distance from Y axis is rc. The thickness of the copper of each hollow turn is tc. Numerical data about the geometry are summarized in Table 1.

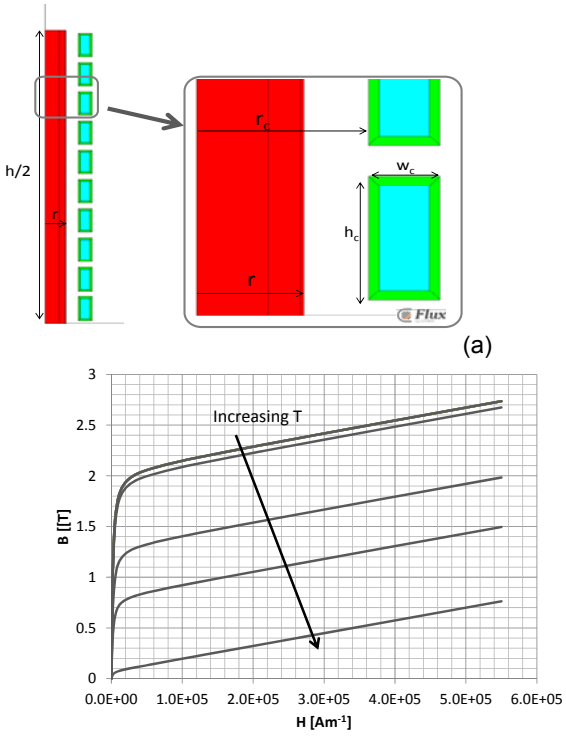

Fig. 1. (a) Geometry of the device, (b) B-H curve dependence on temperature as for Model A.

Table 1. Numerical data about the geometry of the device.

Parameter	Description	Value [cm]
h	Billet height	100
r	Billet radius	3
r_c	Coil internal radius	4.8
h_c	Coil turn height	4
w_c	Coil turn width	2
t_c	Copper turn thickness	0.3

The 20 turns are equally spaced in the Y direction, hence the y-distance between them has to be calculated as (h-20·hc)/19.

a)

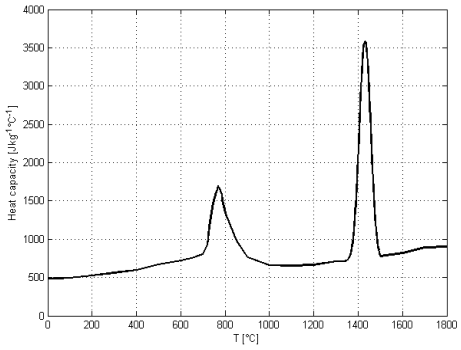

b)

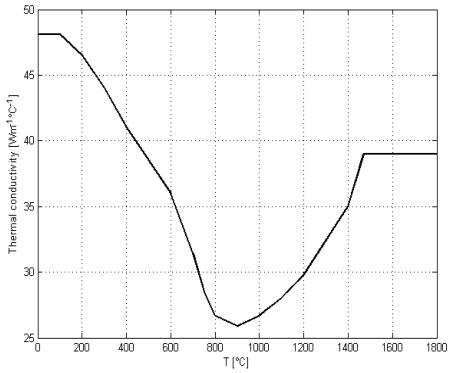

Fig. 2. Material properties of C45 steel: specific heat capacity c_p (a) and thermal conductivity k (b) versus temperature

a)

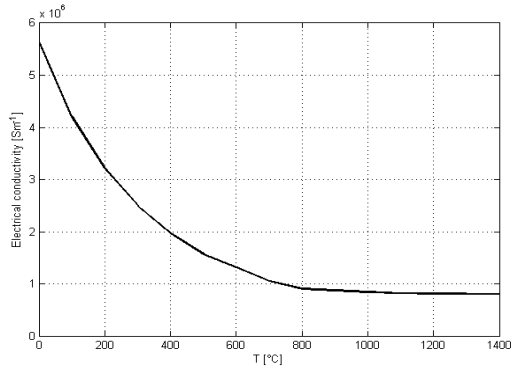

b)

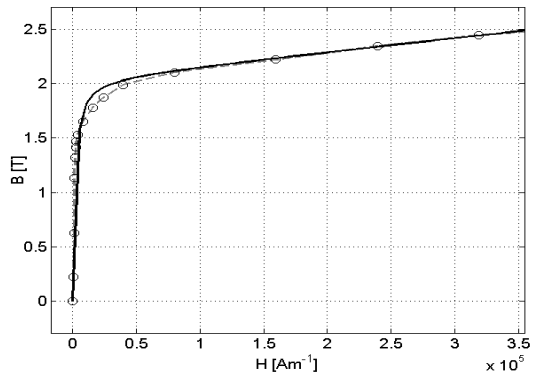

Fig. 3. Material properties of C45 steel: electrical conductivity σ versus temperature (a) and B-H curve at T=20 °C implemented in Model A (dotted gray line), Model B (continous black line), Model C (circle) (b).

B. Material properties

The billet is made of C45 steel, which is characterized by specific heat capacity, thermal conductivity and electrical conductivity, each of them dependent on the temperature, as shown in Figures 2 and 3. Moreover, the B-H curve is dependent on the temperature and this feature is particularly important because in the practical applications of induction heating we are referring to, the transition of magnetic permeability due to the Curie effect is exploited [11]–[15].

Therefore, in the model we propose, a family of temperature-dependent and non-linear B-H curves is considered (see Figure 1 (b).

Three different solvers are used: two of them based on finite element method (MagNet by Infolytica [16] and Flux by Cedrat, Altair, [17]) and one based on finite difference method (ELTA, [18], [19]).

In view of the numerical simulation, different models of the B-H curve can be taken into account; their choice depends on the solver used that could be amenable e.g. to a finite-difference scheme or a finite-element scheme.

In particular, the following three models have been considered:

C. Model A

The relative magnetic permeability μ_r is calculated as follows [11], [20], [21]:

$$\mu_r(T,H) = 1 + f(T)\mu_{BH}(H) \tag{1}$$

where μ_{BH} is the field-dependent relative permeability at T=20°C (Figure 3 b) and Table 2.

Table 2. Relative permeability μ_{BH} at T=20°C.

B[T]	μ_{BH}	B[T]	μ_{BH}
0	0	1.8711	62.3
0.2199	350	1.9906	39.7
0.6283	500	2.1032	21
1.131	600	2.2234	11.1
1.3195	525	2.3436	7.8
1.4137	450	2.4438	6.1
1.4703	390	2.4792	5.5
1.5331	305	2.5539	5.1
1.6487	164	2.6374	4.4
1.7823	89.2	2.7298	3.9

The function f(T) is defined as:

$$\begin{cases} f(T) = 1 - e^{\left(\frac{T-T_c}{C}\right)}, & T < T_1,\ T_1 = T_c C \ln 0.9 \\ f(T) = e^{\left(\frac{10(T_2-T)}{C}\right)}, & T > T_1,\ T_2 = T_1 + 0.1C \ln 0.1 \end{cases} \tag{2}$$

The value of C coefficient has been chosen equal to 20, the Curie temperature T_c = 770 °C.

D. Model B

The relative magnetic permeability μ_r is described by means of its initial value $\mu_{r,i}$ equal to 600, a saturation value of the induction field J_s of 2.05 T and a knee adjusting coefficient a equal to 0.5. Based on this triplet of parameters, the following B-H relationship is assumed [17]:

$$B(H) = \mu_0 H + J_s \frac{H_a + 1 - \sqrt{(H_a+1)^2 - 4H_a(1-a)}}{2(1-a)} \tag{3}$$

with $H_a = \mu_0 H \dfrac{\mu_{r,i} - 1}{J_s}$

The temperature dependence is the same implemented in Model A i.e. equation (2).

E. Model C

The relative magnetic permeability μ_r is modelled as a function of magnetic field H and temperature T as follows:

$$(4)\quad \mu_r(T,H) = 1 + (\mu_r(H) - 1)\left(1 - \left(\frac{T}{T_c}\right)^6\right)$$

where T_c is set to 760 °C.

Benchmark description: the field problem

The electromagnetic and thermal problems can be solved using a 2D axisymmetric model. The electromagnetic problem is solved in time-harmonic conditions, whereas the thermal one is solved in transient conditions with thermal sources is given by the power density induced in the billet. The electromagnetic domain includes half of the inductor, half of the billet and surrounding air, whereas the thermal domain includes only half of the billet; suitable conditions of heat exchange along the boundary are imposed along the billet surface. The inductor is supplied by a sinusoidal current with amplitude equal to 3,500 Arms per turn at frequency 2 kHz.

The source of the thermal problem is the power density dissipated by the eddy currents which arise in the billet.

The electromagnetic and thermal problems are strongly coupled because most of the material properties of C45 steel are temperature dependent and permeability depends both on temperature and field strength; hence,at each time step of the transient thermal analysis, a time-harmonics electromagnetic analysis must be solved. Therefore, despite the simple geometry involved, the field analysis problem is a challenging one.

A. Electromagnetic problem

The electromagnetic 2D problem can be solved using the A-V formulation. The analysis of the magnetic problem is solved in terms of the phasor of the magnetic vector potential, A, coupled with the phasor of the electric scalar potential, V. The following coupled second order PDEs are originated [20], [22]–[24]:

$$(5)\quad \nabla \times \mu^{-1} \nabla \times \dot{A} + j\omega\sigma\dot{A} = -\sigma \nabla \dot{V} + \dot{J}_S$$

and

$$(6)\quad \nabla \cdot \sigma(j\omega \dot{A} + \nabla \dot{V}) = 0$$

with μ material permeability, ω field pulsation, σ electrical conductivity and $\dot{J}$ and $\dot{A}$ are the phasors of the current density and magnetic vector potential, respectively.

Equation (5) is the equation governing the magnetic field, while equation (6) makes the total current to be solenoidal.

Homogeneous Neumann boundary conditions are set along y = 0, while homogeneous Dirichlet conditions are forced elsewhere.

The rectangular air box incorporating the device was truncated at a suitable distance from the device axes.

B. Thermal problem

The thermal problem solves the Fourier equation [10]:

$$(7)\quad \rho c_p \frac{\partial T}{\partial t} - \nabla \cdot (k \nabla T) = \sigma \omega^2 \left\| \dot{\mathbf{A}} \right\|^2$$

with T the unknown temperature, ρ the mass density, c_p the specific heat capacity and k thermal conductivity.

The applied boundary conditions are:

$$(8)\quad n \cdot (k \nabla T) = 0$$ on y = 0 and on x = 0

$$(9)\quad n \cdot (k \nabla T) = h(T_{ext} - T)$$

with h the convective exchange coefficient equal to 7 $Wm^{-2}K^{-1}$ and T_{ext} the external temperature equal to 70°C along lateral surface of the billet (x = r = 3 cm), while T_{ext} = 25°C for the end surface (y = h/2 = 50 cm)

$$(10)\quad n \cdot (k \nabla T) = \varepsilon k_B (T_{ext}^4 - T^4)$$

with ε emissivity coefficient equal to 0.8, k_B the Stefan-Boltzmann constant and T_{ext} = 70 °C for the lateral surface (x = r = 3 cm), while T_{ext} = 25°C for the end surface (y = h/2 = 50 cm).

Methods and numerical solvers

Two different methods are used to solve the field problem: the finite difference method (ELTA code [18], [19]) and the finite element method (MagNet by Infolytica [16] and Flux by Cedrat, Altair, [17]).

For the electromagnetic problem solved with finite element method a 2D second-order mesh has been generated. A typical mesh exhibits 150,000 nodes and 75,000 elements in Flux model, while 775,000 elements in MagNet model. Figure 4 shows a typical mesh in MagNet and a detail of it.

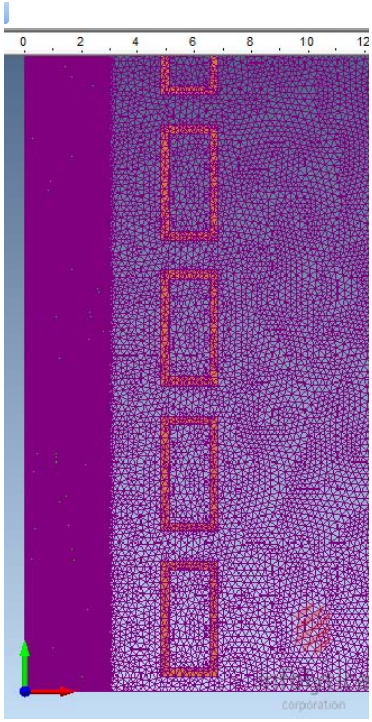

Fig. 4. Typical mesh of the electromagnetic problem in MagNet.

In MagNet and FLUX the conjugate gradient method is used for solving the system of equations from the finite element model. When the matrix system is nonlinear, it has to be linearized before solving the system.

For linearizing the system, the Newton Raphson method is used by MagNet and FLUX. The B-H curves of the C45 steel versus the temperature are supplied to MagNet in the interval from 10 °C to 1500 °C with subintervals of 10 degrees.In each subinterval, the dependence of the B-H curve on the temperature is considered by means of a piecewise linear interpolation. The latter is obtained via a linear regression from equation (2), model A. In Flux the temperature dependent B-H curve is defined using equations (1), (2) and (3). In turn, in ELTA the temperature dependent B-H curve is defined using equation (4).

Solution examples

In Figures 5 and 6 magnetic induction and temperature field maps are shown for time instants t = 12.5 s and t=62.5 s, respectively. The results shown are those obtained by means of Flux.

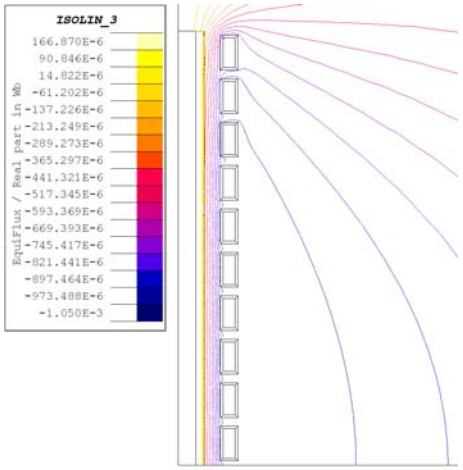

(a)

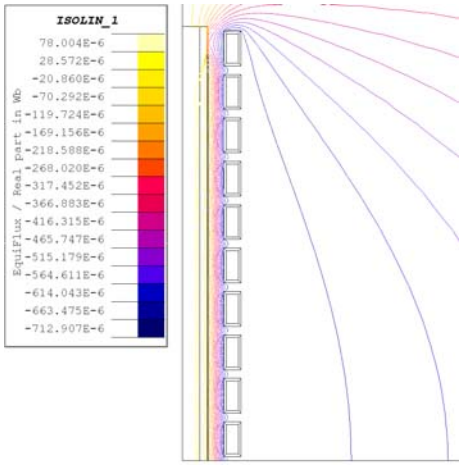

(b)

Fig. 5 Magnetic field maps obtained at t = 12.5 s (a) and t = 62.5 s (b).

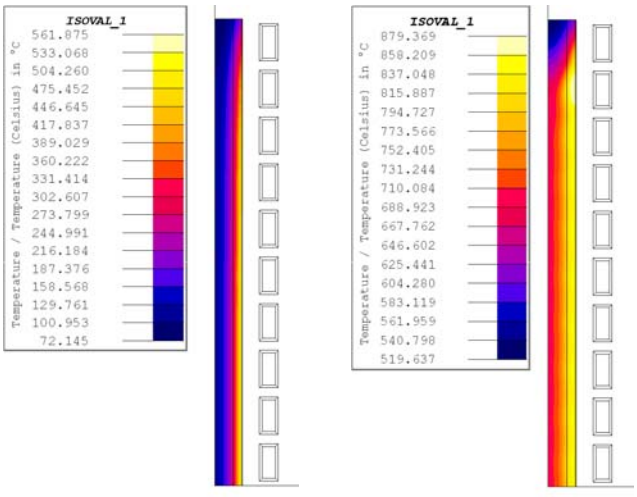

(a) (b)

Fig. 6. Temperature field maps obtained at t = 12.5 s (a) and t = 62.5 s (b).

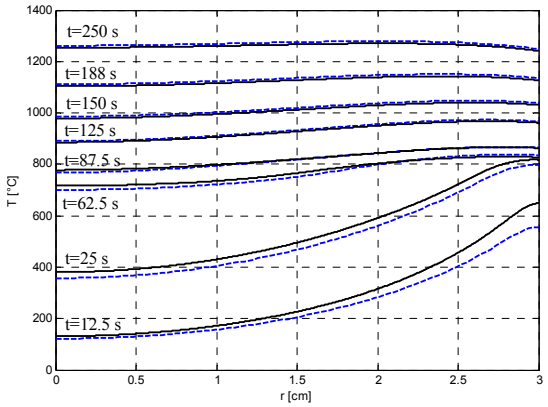

(a)

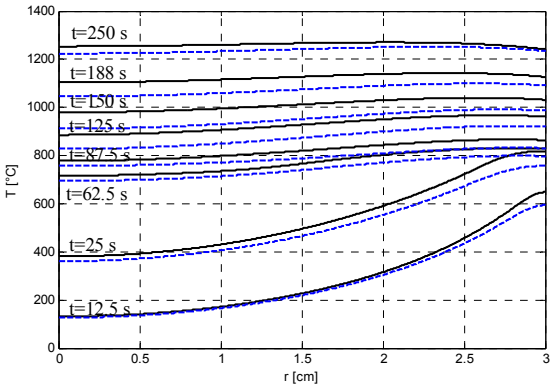

(b)

Fig.7. Temperature versus billet radius at different time instants: (a) MagNet (continuous line) and Flux (dashed line), (b) MagNet (continuous line) and ELTA (dashed line).

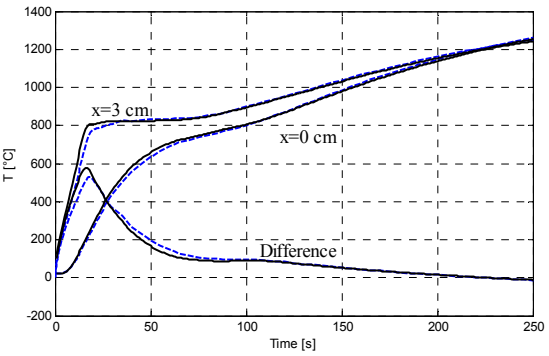

(a)

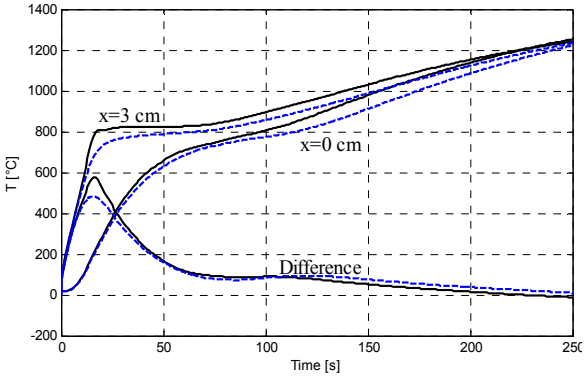

(b)

Fig. 8. Temperature versus time evaluated along the axis (x = 0) and on the billet surface (x = 3 cm), at the middle height of the billet (y = 0): (a) MagNet (continuous line) and Flux (dashed line), (b) MagNet (continuous line) and ELTA (dashed line).

In Figures 7 (a) and 7 (b) the temperature with respect to the billet radius at y = 0 at different times is shown. In particular in Figure 7 (a) a comparison between MagNet and Flux is shown, in Figure 7 (b) the comparison is between MagNet and ELTA.
In Figures 8a and 8b the temperature-time curves are shown. In particular in Figure 8 (a) a comparison between MagNet and Flux is shown, in Figure 8 (b) the comparison is between MagNet and ELTA.

Conclusion

The benchmark problem has made it possible to compare three licensed codes for non-linear field analysis. The obtained results show an acceptable agreement. The computational cost is similar for Finite Element solvers while the Finite Difference solver has proven to be cost effective. The solution of the benchmark by means of other methods, and the comparative analysis of results obtained by different authors are welcome, in order to set up a common ground of research in the area of computational induction heating.

***Authors**: Prof. Paolo Di Barba, Dept. of Electrical, Computer and Biomedical Engineering, University of Pavia, Via Ferrata 5, 27100 Pavia, Italy, E-mail: paolo.dibarba@unipv.it; Dr. Maria Evelina Mognaschi, Dept. of Electrical, Computer and Biomedical Engineering, University of Pavia, Via Ferrata 5, 27100 Pavia, Italy, E-mail: eve.mognaschi@unipv.it; Dr. Marco Bullo, Department of Industrial Engineering, University of Padova, Via Gradenigo 6/A, 35131 Padova, E-mail: marco.bullo@unipd.it; Prof. Fabrizio Dughiero, Department of Industrial Engineering, University of Padova, Via Gradenigo 6/A, 35131 Padova, E-mail: fabrizio.dughiero@unipd.it; Prof. Michele Forzan, Department of Industrial Engineering, University of Padova, Via Gradenigo 6/A, 35131 Padova, E-mail: michele.forzan@unipd.it; Prof. Sergio Lupi, Department of Industrial Engineering, University of Padova, Via Gradenigo 6/A, 35131 Padova, E-mail:sergio.lupi@unipd.it; Dr. Elisabetta Sieni Department of Industrial Engineering, University of Padova, Via Gradenigo 6/A, 35131 Padova, E-mail: elisabetta.sieni@unipd.it;*

REFERENCES

[1] "Testing Electromagnetic Analysis Methods (T.E.A.M.)." [Online]. Available: http://www.compumag.org/jsite/team.html. [Accessed: 11-May-2017].
[2] Di Barba P., Mognaschi M.E., Lowther D.A., Sykulski J.K., A Benchmark TEAM Problem for Multi-Objective Pareto Optimization of Electromagnetic Devices, *IEEE Trans. Magn.*, Article in Press.
[3] Di Barba P., Dughiero F., Forzan M., and Sieni E., Improved solution to a multi-objective benchmark problem of inverse induction heating, *International Journal of Applied Electromagnetics and Mechanics*, 49 (2015), No. 2, 279–288.
[4] Di Barba P., Forzan M., and Sieni E., Multiobjective design optimization of an induction heating device: A benchmark problem, *International Journal of Applied Electromagnetics and Mechanics*, 47 (2015), No. 4, 1003–1013.
[5] Di Barba P., Mognaschi M.E., Lowther D.A. et al., A benchmark problem of induction heating analysis, *International Journal of Applied Electromagnetics and Mechanics*, 53(2017), No. S1, S139–S149.
[6] Di Barba P., Dolezel I., Mognaschi M.E., Savini A., and Karban P., Non-Linear Multi-Physics Analysis and Multi-Objective Optimization in Electroheating Applications, *IEEE Transactions on Magnetics*, 50(2014), No. 2, 673–676.
[7] Di Barba P., Dolezel I., Karban P., Kus P., Mach F., Mognaschi M.E., Savini A., Multiphysics field analysis and multiobjective design optimization: a benchmark problem, *Inverse Problems in Science and Engineering*, 22 (2014), no. 7,1214–1225.
[8] Y. Pleshivtseva, Rapoport E., Nacke B., Nikanorov A. et al., Design concepts of induction mass heating technology based on multiple-criteria optimization, *COMPEL - The international journal for computation and mathematics in electrical and electronic engineering*, 36(2017), No. 2, 386–400.
[9] Pleshivtseva Y., Di Barba P., Rapoport E., Nacke B. et al., Multi-objective optimisation of induction heaters design based on numerical coupled field analysis, *International Journal of Microstructure and Materials Properties*, 9(2014), No. 6, 532–551.
[10] Dughiero F., Forzan M., Pozza C., and Sieni E., A Translational Coupled Electromagnetic and Thermal Innovative Model for Induction Welding of Tubes, *IEEE Transactions on Magnetics*, 48(2012), No. 2, 483–486.
[11] Agarwal P.D., Eddy-current losses in solid and laminated iron, *Transactions of the American Institute of Electrical Engineers, Part I: Communication and Electronics,* 78(1959), No. 2, 169–181.
[12] Kagimoto H., Miyagi D., Takahashi N., Uchida N., and Kawanaka K., Effect of Temperature Dependence of Magnetic Properties on Heating Characteristics of Induction Heater, *IEEE Transactions on Magnetics*, 46 (2010), No. 8, 3018–3021.
[13] Tanaka T. and Homma M., Temperature dependence of the effective permeability of heat treated Sendust alloys, *IEEE Transactions on Magnetics*, 21(1985), No. 4, 1295–1300.
[14] Zedler T., Nikanorov A., and Nacke B., Investigation of relative magnetic permeability as input data for numerical simulation of induction surface hardening, presented at the International Scientific Colloquium Modelling for Electromagnetic Processing, Hannover, 2008, 119–126.
[15] Vladimirov S.N., Zeman S.N., and Ruban V.V., Analytical approximations of thermal dependence of permeability of construction steels," in Proc. of Tomsk univ., 31(2009).
[16] "MagNet 2D/3D Electromagnetic Field Simulation Software | Infolytica Corporation." [Online]. Available: http://www.infolytica.com/en/products/magnet/. [Accessed: 11-January-2018].
[17] "Flux electromagnetic and thermal finite element software." [Online]. Available: http://www.cedrat.com/software/flux/. [Accessed: 11-January-2018].
[18] Nemkov V., Bukanin V., and Zenkov A., Learning and teaching induction heating using the program ELTA., in Proc. HES-10, Padova, Italy, 2010, 99–106.
[19] "Use of the ELTA software for study of electromagnetic and thermal processes in induction heating steel forging lines." [Online]. Available: http://www.nsgsoft.com/contact-us/11-publications/32-practice-of-computer-assisted-design-of-induction-installations-3. [Accessed: 11-January-2018].
[20] Canova A. et al., Identification of Equivalent Material Properties for 3-D Numerical Modeling of Induction Heating of Ferromagnetic Workpieces, IEEE Transactions on Magnetics, 45(2009), No. 3, 1851–1854.
[21] Di Barba P., Komeza K., Juszczak E.N., Lecointe J.P., Napieralski P., and Hihat N., Automated B-H curve identification algorithm combining field simulation with optimisation methods and exploiting parallel computation, *Science, Measurement & Technology, IET*, 6(2012), No. 5, 369–375.
[22] Di Barba P., Savini A., and Wiak S., Field models in electricity and magnetism. [Dordrecht]: Springer, 2008.
[23] Binns K.J., Lawrenson P.J., and Trowbridge C.W, The analytical and numerical solution of electric and magnetic fields. Chichester: Wiley, 1992.
[24] Canova A. et al., Simplified Approach for 3-D Nonlinear Induction Heating Problems, *IEEE Transactions on Magnetics*, 45(2009), No. 3, 1855–1858.